Int. J. Heat Mass Transfer. Vol. 22, pp. 1175–1186
Pergamon Press Ltd. 1979. Printed in Great Britain

TURBULENT FLOW AND PRESSURE LOSSES BEHIND OBLIQUE HIGH-DRAG HEAT EXCHANGERS

F. K. MOORE and J. R. RISTORCELLI, JR.*
Sibley School of Mechanical and Aerospace Engineering, Cornell University,
Ithaca, New York 14853, U.S.A.

(*Received* 14 *April* 1978 *and in revised form* 27 *October* 1978)

Abstract—A theoretical study is made of the flow downstream of very high-drag porous plates aligned obliquely to the ultimate flow direction, representing common oblique heat-exchanger arrangements in dry cooling towers, for example.

Following a brief discussion of the flow between parallel porous plates, the flow in a V-shaped region formed by porous plates is analyzed. It is argued that eddy viscosity increases linearly with distance from the apex, permitting a self-similar solution. Pressure becomes infinite in the apex, and a concentrated jet appears on the centerline; turbulence acts near the centerline to limit the jet velocity there.

Downstream of the V-opening, a narrowing of the flow occurs as it becomes parallel to the centerline, and finally, the velocity profile is fully diffused by turbulence. The velocity profiles, streamline patterns, pressures, and total head losses are fully described for this sequence of flow processes. It is shown that total-head losses can be eliminated by introducing a uniform cascade of airfoils just behind the plates.

NOMENCLATURE

a, maximum value of v/W at centerline;
b, parameter defining streamwise pressure gradient, equation (16);
F, function of ψ, defining vorticity, equation (31);
f, velocity profile function, equation (14);
l, characteristic length for turbulence production;
p, static pressure;
Δp, transverse difference of pressure, from centerline to plate surface;
R_T, turbulent Reynolds number, equation (24);
r, radial coordinate;
U, ultimate leaving velocity parallel to centerline, $W/\sin\theta_0$;
U_s, characteristic velocity defining R_T;
u, velocity parallel to centerline;
v, velocity in radial direction;
W, velocity through porous plates;
w, velocity in θ direction;
x, distance along centerline;
y, distance transverse to centerline; $Y \equiv y/r_s$.

Greek symbols

δ, spacing between parallel plates;
ε, assumed eddy-viscosity coefficient, equation (15);
$\tilde{\varepsilon}$, eddy-viscosity coefficient derived from solution, equation (29);
ν, ν_T, effective or turbulent kinematic viscosity;
ψ, stream function, equations (4) or (30); $\Psi \equiv \psi/Wr_s$;
ρ, density;
θ, angular coordinate (Fig. 3);
θ_0, semi-angle of V-configuration;
Ω, vorticity.

Subscripts

i, ideal pressure just behind bundle, equation (41);
s, at the downstream termination of the bundle (Fig. 3);
0, just behind and along the bundle face (Fig. 3);
1, in parallel separated flow (Fig. 3);
∞, far downstream in uniform flow.

Subscript notation is used for partial derivatives; primes denote ordinary differentiation; and a bar over a quantity signifies an average, either over r or velocity.

INTRODUCTION

IN DRY cooling towers, heat-exchanger bundles are usually arranged in "delta" formations, to conserve space [1, 2]. In some conceptions, the bundles would not be in a delta array, but would be set oblique to the air flow direction [3]. The pressure-loss coefficient based on velocity head normal to the bundle face is typically very large; about 80 for the Grootvlei natural-draft tower [4], and about 40 for that at Rugeley [1]. Consequently, flow features up- and-downstream of the bundle array tend to be rather independent, because the overall driving pressure difference tends to be larger than any possible pressure disturbances in the flow fields.

Nevertheless, severe pressure losses can result from obliquity of the flow, posing important questions of design. Wind, especially, can cause the flow entering a bundle to have large, variable, and uncertain

*Present address: Research Division, Western Electric, Princeton, New Jersey 08540, U.S.A.

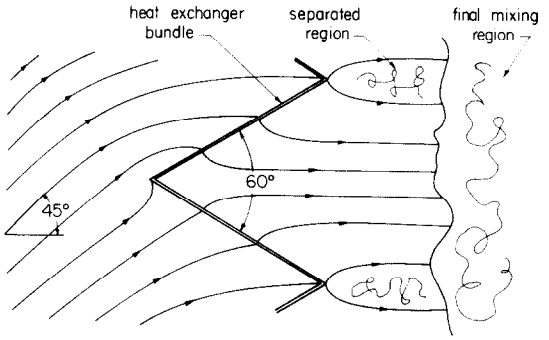

FIG. 1. Sketch of flow through V-bundle, showing streamlines and separated regions.

obliquity relative to the heat-exchanger face. Figure 1 is a composite sketch which illustrates expected flow features for a typical delta array of 60° included angle. Upstream, the flow may be oblique (45° to the axis of the heat-exchanger, in the sketch), owing either to design or to wind. As a result, streamlines will enter the bundle face at very glancing angles, and severe entrance losses will occur. Calculations of these losses are in progress. Downstream, streamlines will emerge from the heat-exchanger in a direction normal to the face, if the overall loss coefficient is high, and then converge into a jet-like flow pattern downstream, with severe separation from the downstream corners. This type of flow pattern is always observed behind heat-exchanger deltas and in laboratory simulations [5]. If a zig–zag screen is placed on a water table, for example, streamline patterns of the sort sketched on Fig. 1 are easily visualized. Large mixing losses are ascribable to the distorted downstream velocity profile shown in the sketch. Although these losses may amount to a significant fraction of the heat-exchanger pressure drop, the engineer has no rational basis for their estimation.

In this paper, an analysis of the turbulent flow downstream of a V-bundle will be developed, giving the pressure variations and streamline patterns in the flow, as well as an estimate of the extra loss coefficients attributable to the V configuration. The width of the separated region will be found. It will be shown that the loss due to an elevated pressure in the V-region itself and that due to the mixing process far downstream are of the same order, with the latter usually predominant. A suggestion will be offered to reduce or even eliminate these effects.

In keeping with the foregoing discussion, the pressure drop across the bundle will be assumed high enough that the emerging normal velocity is essentially constant.

FLOW BETWEEN PARALLEL POROUS PLATES

A starting point for the present analysis is provided by a problem discussed in the review by Raithby [6]. We consider the special case of entry of a uniform flow normally into the region between two parallel porous plates (Fig. 2). This problem is of course not the same as that of a V-bundle, because the bundles do not converge to an apex. However, the parallel-plate problem has a certain relevance to heat-exchanger design, and will certainly illustrate the important role of pressure. Also, flow will be found to concentrate in the centre of the passage, a tendency which will prove to be especially dramatic in the V-bundle case.

If the flow is purely inviscid and incompressible, a simple solution exists [6] for constant W, in which u increases linearly with x, and w is a function only of y.

$$w = -W\sin\pi(y/\delta);\quad u = \frac{\pi W}{\delta}x\cos\pi(y/\delta). \tag{1}$$

The maximum velocity in the middle of the gap is $\pi Wx/\delta$. One should note that this flow, though inviscid, is not irrotational; the vorticity is

$$\Omega = w_x - u_y = \pi^2\frac{Wx}{\delta^2}\sin\frac{\pi y}{\delta}. \tag{2}$$

Static pressure falls in the flow direction at a rate proportional to x^2 and to W^2, and to the narrowness of the gap $1/\delta^2$; the narrower the gap, the higher the pressure gradient must be, in order to turn the flow downstream in that constricted region. Pressure also varies transversely, with the highest level at the center. Denoting p_{max} as the pressure at the center of the upstream face,

$$p = p_{max} - \tfrac{1}{2}\rho W^2\left(\pi^2\frac{x^2}{\delta^2} + \sin^2\frac{\pi z}{\delta}\right). \tag{3}$$

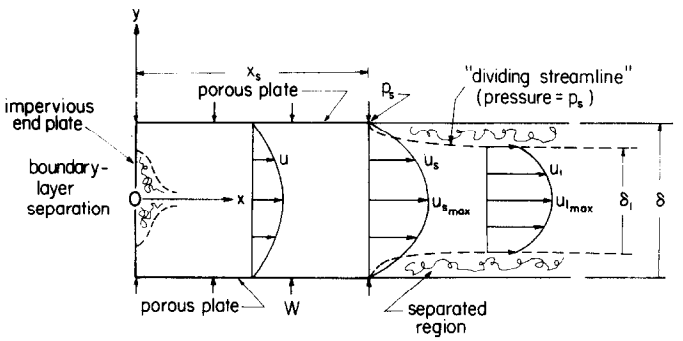

FIG. 2. Sketch of velocity profiles and separation from ends of plates.

We should note that there must be a boundary layer on the forward face, and it must separate, just as at the rear of a cylinder (see Fig. 2). The resulting wake would affect the downstream flow, especially in the center of the gap.

Now, suppose that the plates are terminated at some location x_s bounded by a free surface (Fig. 2) and a constant-pressure separation region forms, bounded by a free surface. We then look for the location of that surface, or "dividing streamline", and for the corresponding velocity profile far downstream. Along any streamline downstream of x_s, vorticity will be constant. At x_s, we may take the stream function to be

$$\Psi_s = Wx_s \sin(\pi y/\delta). \tag{4}$$

Comparing with equation (2), one may therefore write

$$\Omega_s = (\pi/\delta)^2 \psi_s, \tag{5}$$

and the same relationship must hold far downstream where the flow has become parallel. There

$$u_1 = \psi_1'(y); \quad \Omega_1 = -u_1' = \psi_1''(y). \tag{6}$$

Substituting into equation (5) (with subscripts s replaced by subscripts 1),

$$\psi_1'' + (\pi/\delta)^2 \psi_1 = 0. \tag{7}$$

The solution for which pressure and hence velocity are constant along the dividing streamline is

$$\begin{aligned} \psi_1 &= Wx_s \sqrt{1+(\delta/\pi x_s)^2}\, \sin(\pi y/\delta); \\ u_1 &= W(\pi x_s/\delta)\sqrt{1+(\delta/\pi x_s)^2}\, \cos(\pi y/\delta). \end{aligned} \tag{8}$$

In particular, far downstream where $\psi_1 = Wx_s$ and $y = 1/2(\delta_1)$ (see equation (4) and Fig. 2), one must have $u_1 = W$, the resultant velocity at the plate. Also, one finds

$$\frac{\delta_1}{\delta} = (2/\pi)\tan^{-1}(\pi x_s/\delta). \tag{9}$$

From the foregoing results, we may infer that the final width of the flow depends on the length-to-height ratio of the gap, as does the pressure drop from p_0 to the final pressure p_s. In fact, $p_0 - p_s = \frac{1}{2}\rho W^2[1+(\pi x_s/\delta)^2]$.

With heat-exchanger applications in view, the most impressive aspect of these results is the very high pressure drop compared with dynamic pressure of the entering flow, when the heat-exchanger bundles are separated by a distance comparable to or less than their length. For example, if $\delta/x_s = 0.6$, then $(p_{\max} - p_s)/(\frac{1}{2}\rho W^2) = 28.4$. Also, in that case, $(u_s)_{\max}/W = 5.2$, and the final parallel flow has a width of $\delta_1/\delta = 0.88$. These flow features (high back-pressure, and downstream separation) must typically occur when high-resistance bundles are placed oblique to the intended downstream flow direction. In particular, we may expect such effects for the V-bundle arrangement of Fig. 1.

FLOW BEHIND A V-CONFIGURATION

We now return to the problem posed in Fig. 1. The polar coordinate system to be used appears in Fig. 3. For the moment, we imagine that the porous plates at $\theta = \pm\theta_0$ extend to $r = \infty$, and the inward velocity W is constant along them. Thus, we assume that any pressure variations in the downstream flow are so much smaller than the pressure drop across the plates (heat-exchanger bundles) that they do not significantly influence W. In effect, as many practical cases suggest, we assume a very large ratio of the bundle pressure drop to the through-flow dynamic pressure. When applied to the estimation of downstream head losses, our theory should therefore represent the first term of an asymptotic series in that ratio.

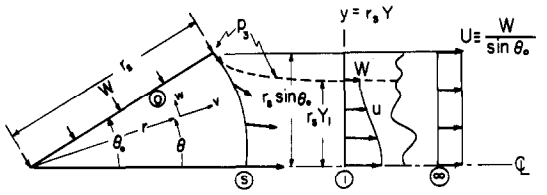

FIG. 3. Sketch of coordinate system and flow processes. Flow becomes parallel between ⓢ and ①, and fully diffused and mixed between ① and ∞.

We may write the equations of viscous motion as follows, with ν representing a kinematic viscosity, for the time being:

$$(rv)_r + w_\theta = 0 \tag{10}$$

$$\begin{aligned} &vv_r + \frac{w}{r}v_\theta - \frac{w^2}{r} + \frac{1}{\rho}p_r \\ &\quad = \nu\left[\frac{4}{3}\left(v_{rr} + \frac{1}{r}v_r - \frac{v}{r^2}\right) + \frac{v_{\theta\theta}}{r^2} + \frac{w_{r\theta}}{3r} - \frac{7w_\theta}{3r^2}\right] \end{aligned} \tag{11}$$

$$\begin{aligned} &vw_r + \frac{w}{r}w_\theta + \frac{wv}{r} + \frac{1}{\rho}\frac{p_\theta}{r} \\ &\quad = \nu\left[w_{rr} + \frac{w_r}{r} - \frac{w}{r^2} + \frac{4w_{\theta\theta}}{3r^2} + \frac{v_{r\theta}}{3r} + \frac{7v_\theta}{3r^2}\right]. \end{aligned} \tag{12}$$

The required boundary conditions are

$$w(r, \pm\theta_0) = \mp W; \quad v(r, \pm\theta_0) = 0. \tag{13}$$

It is natural to try to find a solution in the self-similar form

$$v = Wf'(\theta); \quad w = -Wf(\theta), \tag{14}$$

which would of course satisfy equation (10) identically. For equation (14) to represent a solution of equations (11) and (12), it is clear that rp_r must be constant and ν must be proportional to r. That is,

$$\nu \equiv \varepsilon W r, \tag{15}$$

where ε is a physical parameter, and

$$-\frac{1}{\rho}rp_r = bW^2, \tag{16}$$

Table 1. Results for V-configuration. Boxes enclose solutions consistent with equation (29); that is, $\varepsilon = \tilde{\varepsilon}$

b	ε	θ_0	a	$\frac{\Delta p}{\frac{1}{2}\rho W^2}$	$\tilde{\varepsilon}$	$\frac{Y_1}{\sin\theta_0}$	$\frac{p_i - p_\infty}{\frac{1}{2}\rho U^2}$	$\frac{p_s - p_\infty}{\frac{1}{2}\rho U^2}$	$\frac{\bar{p}_{T_0} - p_{T_\infty}}{\frac{1}{2}\rho U^2}$	$\frac{\bar{p}_{T_s} - p_{T_\infty}}{\frac{1}{2}\rho U^2}$
	0	30.02	∞	0	∞	0.811	0.750	−1.029	0.723	0.723
	0.001	29.98	5.717	0.0107	0.0133	0.811	0.750	−1.017	0.729	0.676
	0.003	29.94	5.244	0.0293	0.0081	0.811	0.751	−1.000	0.737	0.631
5.0	0.006	29.91	4.922	0.0547	0.0060	0.811	0.751	−0.979	0.756	0.589
	0.01	29.88	4.670	0.0861	0.0048	0.811	0.752	−0.953	0.777	0.545
	0.03	29.90	4.076	0.2230	0.0031	0.815	0.752	−0.851	0.883	0.407
	0.05	30.05	3.769	0.3412	0.0025	0.822	0.749	−0.769	0.990	0.326
	0	40.04	∞	0	∞	0.793	0.586	−0.928	0.555	0.555
2.5	0.0041	39.94	3.781	0.0270	0.0041	0.793	0.588	−0.903	0.570	0.485
	0.03	39.89	3.094	0.1569	0.0018	0.796	0.589	−0.806	0.662	0.344
	0	49.45	∞	0	∞	0.792	0.423	−0.802	0.392	0.392
1.4	0.0030	49.46	3.036	0.0147	0.0030	0.792	0.422	−0.792	0.403	0.358
	0.03	49.31	2.478	0.1134	0.0011	0.797	0.425	−0.717	0.467	0.260

where b is a constant. Thus, pressure must fall logarithmically with r, though we should allow for an additive dependence on θ.

The need to make v proportional to r means that the self-similar assumption cannot deal with laminar viscous flow, for which v would be constant. However, flow behind heat-exchangers should be assumed turbulent anyway, and, happily, theory and experiment [7, 8] suggest exactly such a linear relationship for the turbulent jets, wakes and mixing layers with which we would be inclined to compare our flow emerging from linearly diverging walls. The form of equation (15) may be inferred from the idea that turbulent eddies grow in proportion to the width of the flow passage.

However, the value of ε will depend on the wall divergence, and especially on the velocity of the "jet" along the centerline of Fig. 3. This jet velocity is not known *a priori*, and in fact will prove to depend on ε. What we shall do, therefore, is first find solutions for a range of choices of ε, and then find which solution conforms suitably to the treatment of jets and mixing layers provided by Tennekes and Lumley [8].

Proceeding in this way, we use equations (14–16) to transform equations (11–13), which then read:

$$\varepsilon(f''' + f') + ff'' + f^2 + b = 0 \tag{17}$$

$$\varepsilon(f'' + f) - p_0/(\rho W^2) = 0 \tag{18}$$

$$f(\pm\theta_0) = \pm 1; \quad f'(\pm\theta_0) = 0. \tag{19}$$

Clearly, f may be found from equations (17) and (19), with the constant b, initially unknown, constituting part of the solution. Thus, the radial pressure gradient will be found first, and then the azimuthal pressure gradient can be found directly from equation (18).

An "inviscid" solution

It is natural first to look for a solution with $\varepsilon = 0$, as we did for parallel plates. In such a case p is purely a function of r, and equation (17) may be integrated once, after multiplying by f'/f. The result is

$$f'^2 + f^2 - 1 + 2b\ln f = 0, \tag{20}$$

where equation (19) has been applied. The final integration is best done numerically. First, we notice that f' becomes infinite when f vanishes, as it must by symmetry, along the center line $\theta = 0$. In other words, we will find a strong "jet" along the axis.

A series of numerical solutions of equation (20) have been obtained [9] with various values of b ranging from 0.75 to 50. For each value of b, one may find the value of $\theta = \theta_0$ for which $f = 1$ and $f' = 0$. That angle (θ_0) is the semi-vertex angle between the porous plates corresponding to the given pressure gradient (b), when ε is zero. Table 1 and Fig. 4 show that relationship, and the inviscid radial velocity (v) profiles for $b = 5.0$ appears, labeled $\varepsilon = 0$, in Fig. 5.

Figure 4 shows that the pressure gradient goes inversely with vertex angle. Physically, one may say that a more acute vertex angle would mean that the emerging flows from the two sides are more directly opposed, and must turn more abruptly to escape (see Fig. 1). The more abrupt turning must be provided by a stronger pressure gradient. So to speak, a very acute angle tends to trap the entering flow. Figure 4 shows that $b = 5$ corresponds nearly to a semi-angle of 30°, or a heat-exchanger "delta" with a vertex angle of 60°. This is about the lower limit of usual practice.

As we shall see, when turbulent mixing is taken into account, θ_0 will depend on ε, for given b;

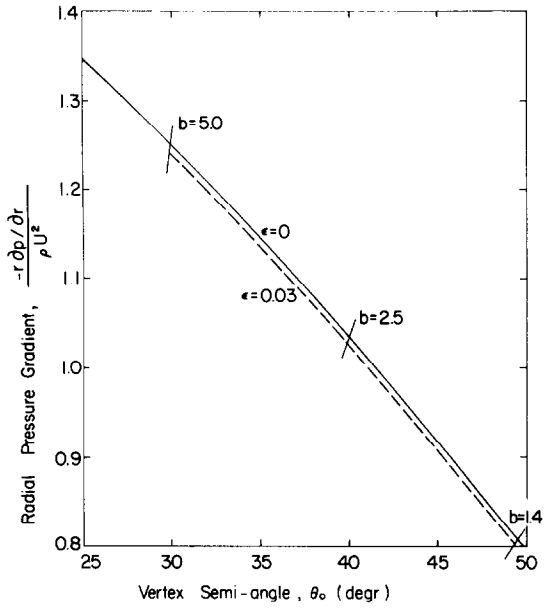

FIG. 4. Streamwise pressure gradient as a function of vertex angle of V-configuration, for no turbulent decay of jet ($\varepsilon = 0$) and for a large decay coefficient ($\varepsilon = 0.03$). Pressure is referred to fully-mixed downstream velocity $U = W/\sin\theta_0$.

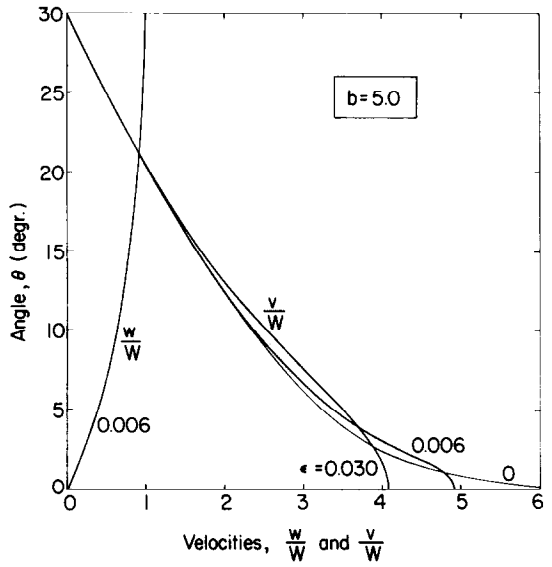

FIG. 5. Profiles of radial (v) and azimuthal (w) velocities for $b = 5.0$ and various assumptions as to the turbulent coefficient ε. It will prove that $\varepsilon = 0.006$ is "correct" for $b = 5.0$.

however, the dependence will prove to be very weak, and the "inviscid" relationship between θ_0 and b will be found to be accurate enough for any practical purpose.

The most distinctive feature of the inviscid solution is the concentrated jet along the plane of symmetry, shown on Fig. 5. In fact, radial velocity goes to infinity as θ goes to zero. In a real flow, there are two phenomena which must actually limit the central flow to finite velocities: the first, which we will study in this paper, is turbulent mixing (finite ε); the second is that the associated high pressure in the vertex will oppose the flow through any real heat-exchanger near the vertex, invalidating our assumption that W is constant everywhere on the surface. Obviously, if flow near the vertex is limited, the downstream "jet" will have finite velocity.

Removing the constant W assumption will generally require consideration of finite-resistance bundles, and hence will also require knowledge of the upstream flow, and abandonment of similarity. These improvements are deferred for subsequent study, and in this paper we will adhere to the assumption that bundle pressure drop is so large that W is constant arbitrarily close to the vertex.

Finally, we should have in mind that real heat-exchangers may have structural features near the vertex which block the flow there. In such a case, the flow will begin like the parallel-plate problem previously described, with finite velocities, and then presumably go over to the similarity solution at large distances from the vertex. This interesting problem, too, we defer for later study.

One may analyze downstream separation and final mixing loss for the inviscid solution. However, we defer this step until after the turbulent-flow problem has been treated.

Asymptotic solution for small ε

If the effect of turbulence is weak (if ε is very small), we may anticipate a boundary layer along the plane of symmetry ($\theta = 0$), wherein v, or $a \equiv v/W$, is quite large but not infinite. Outside this thin turbulent jet, we expect the inviscid solution to apply. If we suppose the turbulent jet to be of angular thickness $\sqrt{\varepsilon}$, so that

$$f = \sqrt{\varepsilon}h(\theta/\sqrt{\varepsilon}), \tag{21}$$

then substitution into equation (17) gives

$$h''' + hh'' + b = 0, \tag{22}$$

to zero order in ε. Now, a solution of the form (21) must be matched to an inviscid solution (equation (20)) at a place where θ is of order $\sqrt{\varepsilon}$, and the inviscid solution must be dominated by the $\ln f$ term, because the layer is very thin. Combining equations (20) and (21) we see directly that, at such a matching point,

$$a^2 \cong -2b(\tfrac{1}{2}\ln\varepsilon + \ln h).$$

Of course, h is of unit order, and we conclude that the asymptotic value of a is

$$a \overset{a}{\cong} [b\ln(1/\varepsilon)]^{1/2}. \tag{23}$$

Therefore, in principle, a is very large if ε is very small. However, we shall find that a reasonable value of ε is about 0.006 and then $[\ln(1/\varepsilon)]^{1/2}$ is only 2.26, which is hardly a large number! Although one may therefore doubt the value of a solution of this problem by asymptotic expansion for small ε, we will find that the exact solution of equations (17–19) for

$b = 5$ and $\varepsilon = 0.006$ gives $a = 4.92$, while the corresponding value obtained from equation (23) is 5.06, only 3% too high.

A more accurate asymptotic procedure would be to solve the inner equation (22) exactly, and match the solution to the inviscid one at some finite θ, requiring the inner solution to give a vanishing value of the left side of equation (20) at the matching point. This procedure will be correct to order ε. However, solution of equation (22) must be done numerically (it is an inhomogeneous Blasius equation, so to speak); thus, one may as well solve the more basic equations (17–19) exactly. The asymptotic formula, equation (23), may be kept in mind as giving a reasonable estimate of jet velocity.

Exact solutions

Equations (17–19) were solved numerically by a finite-difference method for various choices of ε and b. At $\theta = 0$, symmetry requires $f(0) = f''(0) = 0$, and one chooses a trial value of $f'(0)$ (that is, the jet velocity on the axis, a). Then one marches outward in θ until f itself passes through 1. At that point, f' should vanish (the normal exit condition); presumably it does not, and a new value of $a = f'(0)$ is chosen. The process is repeated until $f = 1$ and $f' = 0$ are both true at some θ; that θ is θ_0, the semi-vertex angle which gives the pressure gradient specified by b. The following results were obtained with a step size of $\Delta\theta = 0.0001$, and are accurate to 10^{-6}. Further details appear in [9].

Figure 5 shows how the profile of radial velocity is modified as ε changes, with b held at 5, corresponding to $\theta_0 \cong 30°$. The profile of azimuthal velocity $f(\theta)$ is also shown. It differs only slightly from the inviscid result. As expected, the more turbulent the flow, the lower the radial velocity at the centerline. With θ_0 held fixed, the mass flow must also be fixed. Hence the areas under the various curves of Fig. 5 must be equal. Of course θ_0 changes slightly (Table 1), but the reduction of flow along the axis due to turbulence is nearly compensated for by higher velocities at intermediate angles, and, as Fig. 4 shows, the inviscid relation between b and θ_0 is accurate within 0.4% for all reasonable values of b and ε.

We note that if $\varepsilon = 0.006$ and $\theta_0 = 30°$, the centerline velocity is about 5 times the normal exit velocity at the surfaces (W). The average radial velocity must be W/θ_0 or $1.91W$. Thus, a in this case is about 2.6 times the average radial velocity required by continuity.

Figure 6 shows a as a function of ε. For more open vertex angles (smaller b), the effect of turbulence is more pronounced. The abscissa is scaled in terms of $\sqrt{\ln(1/\varepsilon)}$ to facilitate comparison with equation (23). The asymptotic formula $[b\ln(1/\varepsilon)]^{1/2}$ represents the exact results surprisingly well for all ε values of interest, and for reasonably small vertex angles.

Finally, we note that there is an azimuthal profile of pressure to be derived from equation (18),

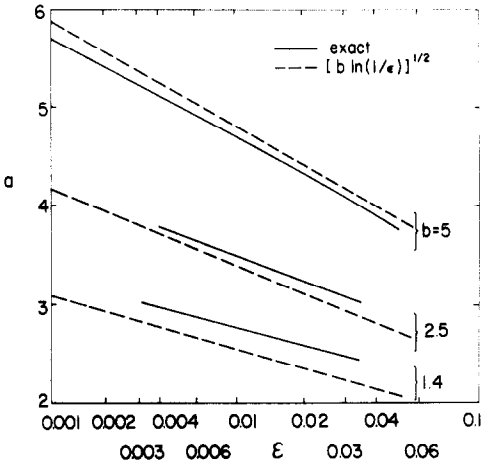

FIG. 6. Maximum velocity on the axis ($a \equiv v_{max}/W$) as a function of turbulence level coefficients (ε) for various pressure gradients or vertex angles. Exact values are compared with a simple formula (equation (23)).

analogous to the transverse pressure variation between parallel plates (equation (3)). The change in pressure between centerline and wall is rather small, of order ε. Table 1 displays values of the excess of pressure between $\theta = 0$ and θ_0 as a coefficient, $\Delta p/(\frac{1}{2}\rho W^2)$. Although $\Delta p/(\frac{1}{2}\rho W^2)$ must be mathematically of order ε, it is typically about 8 times ε in numerical magnitude.

Effective viscosity of turbulence

Having found the velocity structure of our flow behind a porous V-configuration for various values of ε, we are in a position to propose a relationship between our flows and those previously studied, for example by Tennekes and Lumley [8].

Following Chapter 4 of [8], we should choose a length scale l and a velocity U_s to characterize our velocity profile. In so doing, we will be comparing our flow with either a jet or a mixing layer. In our case, it seems more logical to choose the mixing layer; its characteristic velocity U_s is constant as ours should be, whereas the U_s for a jet decreases like $r^{-1/2}$. The essential feature of a mixing layer is that the action is continually forced from the side. This is also true of our flow. A logical difficulty in making the connection between our flow and a mixing layer is that the latter is at constant pressure, whereas we have a radial pressure gradient. However, our gradient dies out with distance, and in any event, the vorticity arising from velocity shear is conserved along these two-dimensional streamlines. Therefore, we feel justified in relating our flow to the two-dimensional mixing or shear layer.

For the plane shear layer, it is recommended [8] that

$$l = \frac{1}{R_T} r; \quad R_T \equiv U_s l/\nu_T = 17.3. \tag{24}$$

This empirical result implies that the transverse scale of mixing is given by an angle of about 3.3°.

Comparing our Fig. 5, we see that our mixing layer is indeed of about that angular dimension. In view of the definition of "Turbulent Reynolds Number" R_T, equation (24) asserts that the eddy kinematic viscosity is proportional to r, provided U_s is constant, as we have assumed. In fact, equations (15) and (24) together yield the value of ε:

$$\varepsilon = \frac{U_s}{W}\frac{1}{R_T^2} = 0.00334\frac{U_s}{W}. \tag{25}$$

It remains to interpret U_s for our problem. For the shear layer, U_s is of course the overall velocity difference [8]. Here, we might think to choose $U_s/W = a$, by analogy. However, we know that much of the velocity change in our problem is unrelated to turbulence. Following a suggestion of Professor Lumley, we note that the significance of U_s is indirect; it is really the velocity gradient which produced the turbulence. Therefore, we define U_s as that velocity which, across a classical shear layer, would cause the same maximum shear as that found in our flow.

The turbulent mixing layer has a velocity profile governed by the equation (4.4.8) of [8], and this equation is actually the classical Blasius equation; the latter, in turn, governs the laminar mixing layer for which the solution was calculated by Chapman [10]. The maximum shear may be found from his results. In our terms,

$$(v_y)_{\max} = 0.736U_s/l, \tag{26}$$

where v_y is a transverse distance coordinate.

In our V-bundle flow, using equation (14), we write

$$(v_y)_{\max} = \frac{1}{r}(v_\theta)_{\max} = \frac{1}{r}W[f''(\theta)]_{\max}. \tag{27}$$

Equating these two expressions for $(v_y)_{\max}$, and using equation (24), we find

$$\frac{U_s}{W} = 0.0785[f''(\theta)]_{\max}. \tag{28}$$

We can find the maximum value of f'' from our numerical solutions (or, roughly, by inspection of Fig. 5). When $b = 5$ and $\varepsilon = 0.006$, the maximum f'' is 22.84, occurring at $\theta = 2.9°$. We note that this value of θ is close to the value of 3.3° associated with the assumption of $R_T = 17.3$, thus giving confidence in the reasonableness of our approach. In this case, U_s/W from equation (28) is 1.79 which is only about 1/3 the overall velocity difference (a).

Finally, then, we substitute equation (28) into equation (25), and obtain our final expression for ε:

$$\tilde{\varepsilon} = 1.359\frac{1}{R_T^3}[f''(\theta)]_{\max} = 2.62\cdot 10^{-4}[f''(\theta)]_{\max}. \tag{29}$$

This quantity is displayed on Table 1. For $b = 5$, the correct value of ε would seem to be 0.006; only for that value is the derived $\tilde{\varepsilon}$ consistent with the ε assumed at the outset. Of course, the coefficient $2.62\cdot 10^{-4}$ is tentative. If it were 10 times as large, then, for $b = 5.0$, the "correct" ε would be 0.03.

For more open angles than 30° ($b < 5.0$), the turbulent intensity may be expected to be less because shear is less. In fact, one finds smaller values of the "correct" ε for the more open angles. As Table 1 indicates, ε for $\theta_0 = 50°$ is only half that for 30°. Figure 7 shows the "correct" profiles for 30, 40 and 50°.

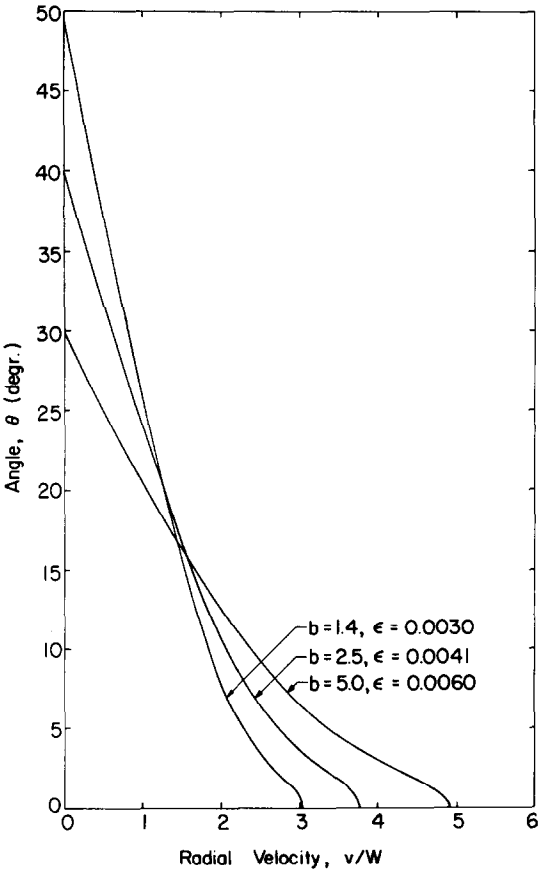

FIG. 7. Radial velocity profiles for three vertex angles and corresponding pressure coefficients (b), each for the correct turbulence coefficient (ε) according to equation (29).

Experiments have recently been performed at Oxford University [5] which apparently give credence to the velocity profiles described here, although the measurements of centerline velocity may perhaps imply larger values of ε than those found to be "correct" in this study.

Downstream separation

Just as we did in the simpler case of parallel plates, we may now imagine the V array to terminate at r_s, where separation will then occur. We adopt the simple, classical "free-surface" model for separation [11], wherein a constant-pressure dead-water region of finite extent is bounded by a dividing streamline of constant velocity (because pressure is constant). Far downstream from the corner at r_s, we consider that the flow becomes a parallel shear flow, necessarily at the same pressure as that at separation and in the

separated zone. We ignore the actual process, except to assume it is inviscid; we only ask, what is the final velocity profile, and what is the width of the separated region? This process is indicated on Fig. 3 as occurring between the stations Ⓢ and ①. We imagine that a final turbulent decay process then follows the flow-straightening phase, with the parallel flow being mixed with the separated "dead water", so that uniform flow is ultimately achieved at ② as illustrated in Fig. 3.

As in the parallel-plate case, we begin by identifying the vorticity and stream function at r_s; they are

$$\Omega = \frac{W}{r_s}[f''(\theta)+f]; \quad \psi = Wr_s f. \tag{30}$$

In any given case, from numerical results we can tabulate a function $F(f)$:

$$f''+f \equiv F(f), \tag{31}$$

so that $\Omega = (W/r_s)F(\psi/Wr_s)$. Now, far downstream, where $\Omega = u_y$ and $u = \psi_y$ (y being measured perpendicular to the centerline and u being parallel to the centerline), the same $\Omega(\psi)$ relationship must hold in an inviscid flow. Thus, in dimensional terms (defining $Y \equiv y/r_s$ and $\Psi \equiv \psi/Wr_s$),

$$\Psi_{YY} = F(\Psi). \tag{32}$$

This constitutes a differential equation for Ψ, subject to the boundary conditions that $u = W$ far downstream on the dividing streamline (because we hold pressure constant along that streamline), and that the stream function continues to vanish on the centerline:

$$\Psi_Y = 1 \text{ when } \Psi = 1; \quad \Psi = 0 \text{ when } Y = 0. \tag{33}$$

A general solution of equation (32) may be obtained by multiplying by Ψ_Y and integrating with respect to Ψ. Then, application of the boundary conditions, equations (33), yields

$$Y = \int_0^{\Psi} \left[1 - 2\int_{\Psi}^{1} F(\Psi)\,d\Psi\right]^{-1/2} d\Psi. \tag{34}$$

Knowing $F(\Psi)$, one can find the downstream profile function $\Psi(Y)$ from equation (34). In the inviscid case, $\varepsilon = 0$, equations (17) and (31) tell us that $F(f) = -b/f$. Equation (34) then gives

$$Y = \sqrt{\frac{\pi}{2b}}\, e^{1/2b}\,\mathrm{erfc}\left[\frac{1}{2b} - \ln\Psi\right]^{1/2}, \tag{35}$$

whence the inviscid downstream profile and the corresponding width of the downstream flow may be found:

$$\frac{u}{W} = \Psi_Y = [1 - 2b\ln\Psi]^{1/2} \tag{36}$$

$$Y_1 = \sqrt{\pi/2b}\, e^{1/2b}\,\mathrm{erfc}\sqrt{1/2b}. \tag{37}$$

When the flow is turbulent upstream of separation, it is a simple matter to evaluate equation (34) by numerical integration.

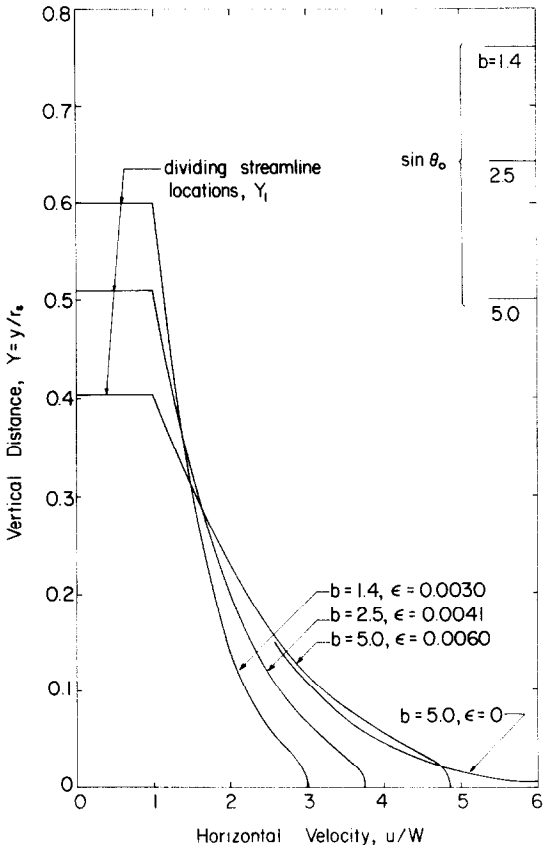

FIG. 8. Velocity profiles at station ①, following the inviscid straightening process. These profiles should be compared with those for radial velocity at Ⓢ, shown in Fig. 7, and the inviscid profile shown in Fig. 5.

We should recall that when ε is not zero, there is an azimuthal pressure gradient of that order. It proves impossible to accommodate this effect in the sequential flow calculation just described. Thus, equation (34) surely embodies an error of order ε; however, that does not prevent us from including features of the jet at station Ⓢ such as the maximum velocity a, which is of lower order, $[\ln(1/\varepsilon)]^{1/2}$.

Figure 8 gives the profile of downstream u/W for $\varepsilon = 0$ and $b = s$, obtained from equation (36). Also shown are the profiles for several wedge angles and the corresponding "correct" values of ε. Table 1 shows the streamline contraction in terms of the ratio $Y_1/\sin\theta_0$ (see Fig. 3). The contraction is nearly independent of ε, and is nearly 20% of the rear opening of the V, whatever the vertex angle. These results may be compared with those presented earlier for parallel plates.

It is not certain that the process Ⓢ--① may properly be considered inviscid, especially if the flow up until Ⓢ is taken to be turbulent. In effect, we have assumed a two-step process in which, at first, vorticity has no chance to diffuse in the short interval necessary to adjust flow direction by pressure forces following separation, and second, turbulent diffusion accomplishes final decay of vorticity on a much longer time scale. It appears that the present

predictions of separated-zone width are rather well confirmed by recent experiments by Jones already mentioned [5].

Pressure effects and losses

It remains to calculate the pressure losses attributable to the V configuration. We shall refer to the sketch of Fig. 3 which summarizes the steps of the process.

After the shear flow is established at ①, as described in the last section, there will be a final mixing process, which in fact might not be completed in a given cooling tower. However, it would be desirable if it should, because a degree of pressure recovery would occur. A momentum balance between ① and ⑳ gives

$$\frac{p_s-p_\infty}{\frac{1}{2}\rho U^2}=2\left[1-(\sin\theta_0)\int_0^{Y_1}\left(\frac{u}{W}\right)^2 dY\right]. \quad (38)$$

We will refer all pressure differences to the dynamic pressure of the fully-mixed flow at infinity, $U = W/\sin\theta_0$. According to equation (16), the pressure in the V-region is given by

$$\frac{p_0-p_s}{\frac{1}{2}\rho U^2}=2b(\sin^2\theta_0)\ln(r/r_s), \quad (39)$$

and the average of this pressure coefficient over the bundle face is

$$\frac{\bar{p}_0-p_s}{\frac{1}{2}\rho U^2}=2b\sin^2\theta_0. \quad (40)$$

Next, we define a fictitious ideal pressure p_i to be that which would be needed at the surface if the entering flow (W) were turned and accelerated to the condition at ⑳ in a smooth, loss-free channel or nozzle. From Bernoulli's equation, $p_i+\frac{1}{2}\rho W^2 = p_\infty + \frac{1}{2}\rho U^2$, we find

$$\frac{p_i-p_\infty}{\frac{1}{2}\rho U^2}=\cos^2\theta_0. \quad (41)$$

This is the minimum pressure drop associated with turning the flow downstream. Owing to losses, the actual average pressure drop $\bar{p}_0-p_\infty$ will be larger, as we shall see.

Any pressure difference of interest may be constructed from the foregoing set. Table 1 presents coefficients describing p_i and p_s. In general, the integration needed in equation (38) can best be done numerically, although when $\varepsilon = 0$, an analytical solution can be found by use of equations (35) and (36):

$$\left(\frac{p_s-p_\infty}{\frac{1}{2}\rho U^2}\right)_{\varepsilon=0}=2\left[1-(\sin\theta_0)\left(1+\sqrt{\frac{\pi b}{2}}e^{1/2b}\operatorname{erfc}\sqrt{\frac{1}{2b}}\right)\right]. \quad (42)$$

It is customary and convenient to express the configurational losses of interest in terms of total head. Head loss occurs in two stages, the first of which is the turbulent decay of the jet near the centerline; this loss is realized before station ⑤. From ⑤ to ①, a flow adjustment occurs with, we assume, no loss. The second loss occurs between ① and ⑳ where turbulent mixing smooths out the velocity profile.

We define average total head as the total flux of mechanical energy $p+(\frac{1}{2}\rho u^2)$, divided by the volume flow, at each station. Thus, average total head will be the velocity-averaged total pressure. Along the porous surface ⓪, the average total pressure can be obtained simply by adding the entering dynamic heat ($\frac{1}{2}\rho W^2$) to equation (40):

$$\frac{\bar{p}_{T_0}-p_s}{\frac{1}{2}\rho U^2}=(1+2b)\sin^2\theta_0. \quad (43)$$

In the ultimate mixed condition, where the velocity is again constant (U), the average total head is simply given by $(\bar{p}_{T_\infty}-p_\infty)/\frac{1}{2}\rho U^2 = 1$. Therefore, the overall loss of total head from ⓪ to ⑳ is

$$\frac{\bar{p}_{T_0}-p_{T_\infty}}{\frac{1}{2}\rho U^2}=(1+2b)\sin^2\theta_0-1+\frac{p_s-p_\infty}{\frac{1}{2}\rho U^2}, \quad (44)$$

where the last term is supplied by equation (38) (or (42), if $\varepsilon = 0$). Table 1 and Fig. 9 show values of this overall loss behind the bundles.

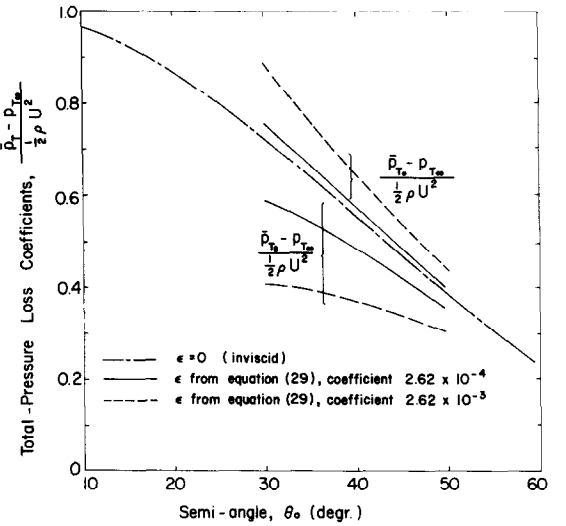

FIG. 9. Total-head losses in numbers of leaving dynamic heads; overall from ⓪ to ⑳, and in the final mixing process ① to ⑳. The latter is the same as from ⑤ to ⑳ because loss from ⑤ to ① has been neglected.

At the intermediate stage ⑤, the flux of mechanical energy (unchanged between ⑤ and ①) is

$$r_s\int_0^{Y_s}(p_s+\tfrac{1}{2}\rho u^2)u\,dY.$$

Manipulation of this expression yields a formula for head loss between ⑤ and ⑳, again relying on equation (38) to evaluate the last term:

$$\frac{\bar{p}_{T_s}-p_{T_\infty}}{\frac{1}{2}\rho U^2}=(\sin^2\theta_0)\int_0^{Y_1}\left(\frac{u}{W}\right)^3 dY-1+\frac{p_s-p_\infty}{\frac{1}{2}\rho U^2}. \quad (45)$$

Results are shown in Table 1 and Fig. 9.

Figure 9 displays the essential results of our analysis of losses. First, we note that use of the inviscid solution, equation (42), to evaluate equations (44) and (45) gives a good indication of the magnitude of the overall loss (about 3/4 of the dynamic head leaving the configuration, if $\theta_0 = 30°$) and the trend to smaller losses for more open angles. If $\varepsilon = 0$, the "jet" is inviscid, and all the loss is ascribable to the final mixing from ① to ②.

The solid lines show the turbulent calculations for the correct values of ε based on equation (29). One sees that the overall loss is only slightly greater, at least for moderate vertex angles, but the final mixing loss is less than the inviscid value. The difference, $\bar{p}_{T_0} - \bar{p}_{T_s}$, is the jet-decay loss from ⓪ to ⓢ. Clearly, this jet loss is predicted to be a small fraction of the overall loss. In other words, the final mixing loss is the primary mechanism of concern.

The dashed lines show how results would change if our estimate of the Turbulent Reynolds Number were badly in error. If the coefficient of equation (29) were increased by a factor of 10 (that is, if R_T were decreased from 17.3 to 8.0), then the overall loss would be greater, and the jet loss would be about equal to the final mixing loss.

Before closing this summary of losses, we should emphasize that our assumption of infinite pressure drop through the bundles themselves, made in order that W be constant, masks another loss which is practically important, and which must be considered in the next phase of our study. That loss will occur because the r-dependence of p_0 means that W will also depend on r if pressure-drop is finite, and this maldistribution of inflow will be adjusted by mixing, just as the profile at ① becomes uniform at ②, and total head will consequently be lost.

The elimination of head loss

As we have shown, head loss is a measure of failure to achieve p_i behind the bundles. Conversely, p_i is the lowest back pressure that can be achieved when the low-velocity stream W is accelerated to the entrance velocity U. One would like, therefore, to have an ideal nozzle with gradual contours all the way from the bundle exit ⓪ to the tower entrance condition ②. Clearly, a gradual nozzle is not topologically possible given the geometrical constraints of the V-bundle. Equally clearly, the only way to make a geometrically compatible nozzle is to introduce a cascade of airfoils designed to turn the flow abruptly with minimum loss, just as in the first-stage stator of an axial-flow turbine. Such a cascade is sketched in Fig. 10. The flow immediately downstream of the cascade would now be in the proper direction, with the proper velocity (U) to proceed without further loss into the cooling tower. The pressure, ideally, will be p_i. In effect, the force needed to turn the flow from the bundle would be provided by the structure supporting the cascade, rather than by a high pressure resulting from the collision of opposing air streams.

For abrupt turning, it is crucial that the cascade have a short chord, and hence a close spacing. Probably the cascade should be mounted directly on the bundle as a sort of last row of the heat exchanger. It is also crucial that the cascade provide uniform turning, especially near the apex; otherwise, the pressure there would be very large.

A cascade will have a certain flow-turning efficiency (as a fraction of the turning angle of the airfoils themselves) which depends on solidity (chord-to-gap ratio). There is a compromise to be made here, because a very high-solidity cascade will itself suffer drag losses which would defeat its present purpose. Figure 10 shows that even if the turning efficiency of the cascade (expressed as the ratio of

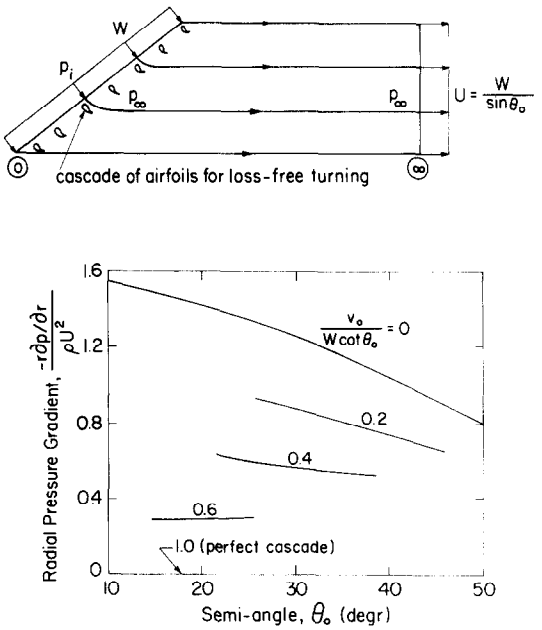

FIG. 10. An airfoil cascade to reduce pressure loss. A "perfect" cascade is sketched, and pressure gradient is shown as a function of efficiency $v_0/(W\cos\theta_0)$, calculated for $\varepsilon = 0$. For no cascade, efficiency is 0, and pressure gradient is as in Fig. 4; for a perfect cascade, efficiency is 1.0, and radial pressure gradient vanishes.

radial velocity achieved compared with that necessary to make the flow parallel to the centerline) is rather poor, there will be a substantial reduction of radial pressure gradient for a given V-angle. For example, if $\theta_0 = 30°$ and the cascade turning efficiency is only 30%, the pressure gradient is reduced by 35%, to nearly the level expected for a wider V of semi-angle 50° with no cascade.

Clearly, even an inefficient cascade should be most effective in reducing configurational losses for oblique heat-exchangers, not only for V-arrangements, but for any arrangement which entails turning of the flow emerging from the bundle face. Further research will be needed to discover the optimum degree of refinement for the cascade design.

In closing, we should note that the postulated cascade will also eliminate at least part of an additional loss not considered in this paper, namely the mixing loss due to any nonuniformity of W caused by nonuniform pressure difference across the bundles.

CONCLUSIONS

A theoretical study has been made of the flow downstream of very high-drag porous plates aligned obliquely to the ultimate flow direction. The flow emerging from the porous plates was then assumed to be of constant velocity, normal to the surfaces, everywhere on the surfaces. The porous plates represent the downstream surfaces of heat-exchanger bundles of the sort used in dry cooling towers. The basic purpose of the study has been to analyze certain sources of head loss assignable to the oblique configuration, and thus to find means to reduce such losses.

First, the well-known flow between parallel porous plates was reviewed and extended for the present purpose. The arrangement is terminated upstream by a solid end-plate, and downstream by abrupt edges. The flow was assumed inviscid, and it was shown that an extremely high pressure may be expected on the end plate, with pressure decreasing toward the open end. Also, a stagnant separation region may be expected on the end plate itself. For a "square" arrangement, the maximum over-pressure is about $2\frac{1}{2}$ leaving dynamic heads, representing an extra draft requirement. If the plates are more closely spaced, the over-pressure is greater. Downstream of the plate ends, separation is represented by a constant-pressure free streamline. This dividing streamline leads to a parallel flow, still having a parabolic velocity profile, but narrowed to about 80% of the width of the original stream.

The more extensive part of this study concerns the flow behind a V-bundle, for which the porous plates are joined upstream. An inviscid analysis shows a self-similar flow with logarithmically infinite pressure at the apex, and a concentrated jet along the centerline between the plates. The average pressure on each plate exceeds the final static pressure by about $1\frac{1}{2}$ final dynamic heads, for a V-semi-angle of 30°.

The concentrated jet is diffused by turbulence near the centerline, and it proves possible to accommodate in the analysis the assumption that eddy viscosity increases linearly with radius; by reference to two-dimensional mixing-layer information, this seems a correct approach. Eddy viscosity then provides that the maximum centerline velocity is about twice the average final leaving velocity (U), for a semi-angle of 30°. This smoothing of the centerline jet occurs in a narrow zone near the centerline, and entails a loss of average total head of about 1/5 the final dynamic head. The maximum velocity is lower for more open angles or greater turbulent intensity.

Constant-pressure separation is assumed beyond the plate ends, leading to parallel flow, with a calculated velocity profile, narrowed to about 80% of the V opening. This non-uniform but parallel velocity profile may further decay, ultimately to a uniform flow far downstream. In this process, a further loss of total head occurs, amounting typically to 3/5 of final dynamic head for a semi-angle of 30°.

The importance of the high pressure near the V-apex has been emphasized, and it has been pointed out that the overall total-head loss ascribable to the V configuration is equal to the difference between the average face pressure and the Bernoulli pressure needed only to accelerate the flow from the heat-exchanger to the final leaving condition. This configurational loss can be eliminated in principle by introduction of a uniform cascade of airfoils at the exit surface of each bundle, designed to turn the flow immediately to the proper ultimate direction. The cascade must extend to the apex, and should have a high solidity; however, it was shown that even a rather inefficient cascade will be very effective in reducing total head loss.

Subsequent studies should concern the losses associated with oblique entrance to heat-exchangers, and then the effects of losses in causing maldistribution of flow through the bundles themselves.

Acknowledgement—This research was supported by the National Science Foundation (Heat-Transfer Program of the Engineering Division) through Grant No. ENG76-02516.

REFERENCES

1. P. J. Christopher and V. T. Forster, Rugeley dry cooling tower system, *Proc. Inst. Mech Engng* **184**, 197–221 (1969–70).
2. R. C. Norton, W. J. Westre and G. L. Larsen, Dry cooling design characteristics of a large power plant, *Proc. Am. Power Conf.*, Vol. 37, pp. 591–597, Ill. Inst. Tech., Chicago (1975).
3. C. M. B. Russell, T. V. Jones, D. W. Holder, H. R. McChesney and M. Verlinden, Cross wind and internal flow characteristics of dry cooling towers, *Proc. Am. Power Conf.*, Vol. 39, pp. 709–718, Ill. Inst. Tech., Chicago (1977).
4. N. T. Van der Walt, L. A. West, T. J. Sheer and D. Kuball, The design and operation of a dry cooling system for a 200 MW Turbo-Generator at Grootvlei power station, South Africa. Presented at 9th World Energy Conf., Detroit, Mich. Sept. 22–27 (1974).
5. T. V. Jones, Oxford University, private communication; also forthcoming paper by T. V. Jones and C. M. B. Russell of C. E. Lummus Co.
6. G. Raithby, Laminar heat transfer in the thermal entrance region of circular tubes and two-dimensional rectangular ducts with wall suction and injection, *Int. J. Heat Mass Transfer* **14**, 223–243 (1971).
7. H. Schlichting, *Boundary-Layer Theory*, Ch. XXIV (Translated by J. Kestin), McGraw-Hill, New York (1968).
8. H. Tennekes and J. L. Lumley, *A First Course in Turbulence*, M.I.T. Press, Cambridge (1972).
9. J. R. Ristorcelli Jr., Turbulent flow profiles and pressure losses downstream of high drag wedge-shaped heat-exchangers, M.S. Thesis, Cornell University (1978).
10. D. R. Chapman, Laminar mixing of a compressible fluid, NACA Report 958, U.S. Govt Printing Off. (1950).
11. H. Lamb, *Hydrodynamics*, 6th ed., Arts. 73–77, Dover (1946).

ECOULEMENT TURBULENT ET PERTES DE CHARGE DANS UN ECHANGEUR DE CHALEUR OBLIQUE A FORTE TRAINEE

Résumé—On étudie théoriquement l'écoulement à travers des plaques poreuses à forte traînée alignées obliquement suivant la direction ultime de l'écoulement, ce qui représente les arrangements d'un échangeur de chaleur oblique, par exemple dans les tours de lyophilisation.

Après discussion sur l'écoulement entre plaques parallèles poreuses, on considère l'écoulement dans une région en dièdre formée par les plaques poreuses. On admet que la viscosité turbulente augmente linéairement avec la distance à l'arête, ce qui permet une solution en similitude. La pression devient infinie sur l'arête et un jet concentré apparaît sur la ligne centrale; la turbulence agit près de la ligne centrale pour limiter la vitesse du jet.

En aval de l'ouverture en V, un rétrécissement de l'écoulement se fait parallèlement à la ligne centrale et finalement le profil de vitesse est entièrement diffusé par turbulence. Les profils de vitesse, les configurations d'écoulement, les pressions et les pertes de charge totales sont complètement décrits dans ce cas d'écoulement. On montre que la perte de charge totale peut être éliminées en introduisant une cascade uniforme de profils juste derrière les plaques.

ТУРБУЛЕНТНОЕ ТЕЧЕНИЕ И ПОТЕРИ ДАВЛЕНИЯ НА ВЫХОДЕ ИЗ НАКЛОННО РАСПОЛОЖЕННЫХ ТЕПЛООБМЕННЫХ УСТРОЙСТВ С БОЛЬШИМ КОЭФФИЦИЕНТОМ СОПРОТИВЛЕНИЯ

Аннотация — Проведено теоретическое исследование течения за пористыми пластинами с очень высоким коэффициентом сопротивления, помещенными под углом к направлению потока. Такая конфигурация является типичной для теплообменников, используемых, например, в сухих градирнях.

Вначале кратко рассмотрен случай течения жидкости между параллельными пористыми пластинами, после чего дан анализ течения в V-образной области, образованной пористыми пластинами. Показано, что вихревая вязкость возрастает линейно с увеличением расстояния от угла вершины, что следует из автомодельного решения. Величина давления вблизи вершины становится бесконечной, а на геометрической оси конфигурации появляется сконцентрированная струя. Влияние турбулентности вблизи геометрической оси сводится к ограничению скорости струи в этой области. За входом в V-образную область происходит сужение потока; течение становится параллельным геометрической оси, и, в конечном итоге, профиль скорости полностью размывается турбулентностью. Для этой последовательности процессов течения дано подробное описание профилей скорости, линий тока, изменения давления и суммарных потерь напора. Показано, что суммарные потери напора могут быть исключены за счёт установки непосредственно за пластинами решётки равномерно распределенных профилей.

TURBULENTE STRÖMUNG UND DRUCKVERLUSTE HINTER SCHRÄG ANGEORDNETEN WÄRMEÜBERTRAGERN MIT HOHEM STRÖMUNGSWIDERSTAND

Zusammenfassung—Die Strömung hinter einer porösen Platte mit hohem Strömungswiderstand, die schräg zur endgültigen Strömungsrichtung ausgerichtet ist, wird in einer theoretischen Studie untersucht. Der Aufbau entspricht zum Beispiel gewöhnlichen, schräg angeströmten Wärmeübertrageranordnungen in Trockenkühltürmen.

Im Anschluß an eine knappe Betrachtung der Strömung zwischen parallelen, porösen Platten wird die Strömung in einer V-förmigen Zone, die durch poröse Platten gebildet wird, untersucht. Es wird angenommen, daß die scheinbare Zähigkeit mit der Entfernung vom Scheitelpunkt linear zunimmt, woraus sich die Möglichkeit der Ähnlichkeitslösung ergibt. Im Scheitelpunkt wird der Druck unendlich hoch, und in der Mittelachse bildet sich ein scharfer Strahl, wobei die Strahlgeschwindigkeit inin der Nähe der Mittelachse durch die Turbulenz begrenzt wird. Hinter der Öffnung der V-förmigen Anordnung, wo die Strömung parallel zur Mittelachse verläuft, tritt eine Einschnürung ein, und schließ lich wird das Geschwindigkeitsprofil durch die Turbulenz vollständig ausgeglichen. Die Geschwindigkeitsprofile, Stromlinienformen, Drücke und Austrittsverluse werden für diese Folge von Strömungsvorgängen vollständig beschrieben.

Es wird gezeigt, daß die Austrittsverluste durch den Einsatz von Schaufelgittern gleich hinter den Platten beseitigt werden können.